



IR photodissociation spectroscopy of O_4^+ , O_6^+ and O_8^+ cluster ions

A.M. Ricks, G.E. Doublerly, M.A. Duncan*

Department of Chemistry, University of Georgia, Athens, GA 30602-2556, United States

ARTICLE INFO

Article history:

Received 25 November 2008

Accepted 20 January 2009

Available online 30 January 2009

Keywords:

Ion spectroscopy

Clusters

Infrared

ABSTRACT

O_4^+ and larger $(O_2)_n^+$ cluster ions are produced in a pulsed discharge source and studied with time-of-flight mass spectrometry and infrared laser photodissociation spectroscopy. The infrared laser photon energies used allow bracketing of the cluster dissociation energies. Sharp resonant structure is detected for each of these ions in the region of the O–O stretching vibrations and also at higher frequencies corresponding to combination bands. Although previous matrix isolation spectroscopy on O_4^+ found evidence for both *trans*-bent and rectangular isomers of this ion, the gas phase IR spectrum only contains bands assigned to the rectangular isomer. O_6^+ has a distinctive IR spectrum unlike that for O_4^+ , indicating that it is not simply a solvated O_4^+ species, while O_8^+ has the signature of a solvated O_6^+ ion.

© 2009 Elsevier B.V. All rights reserved.

1. Introduction

O_4^+ molecular ions are implicated in the ion chemistry of the earth's atmosphere, serving as intermediates in the formation of protonated water clusters in the "D" region of the lower ionosphere [1,2]. An ion of mass 64 has been detected in airborne mass spectrometry in this region and assigned to O_4^+ [3]. These cations have also been well studied in laboratory mass spectrometry, where numerous reaction pathways and rates have been documented [4–14]. Various methods have been employed to determine the dissociation energies of $(O_2)_n^+$ ions [4,5,15–18]. Electronic photodissociation spectroscopy in the gas phase has investigated the excited states of O_4^+ [19–22]. The ground state spectroscopy of this ion has been studied via EPR [23] and infrared measurements [24–26] for the ions isolated in cryogenic rare gas matrices. Attempts by theory to assign the experimental spectra have revealed the complexity of the electronic structure and bonding in O_4^+ . Consequently, this ion has been the subject of several computational chemistry studies focusing on the symmetry breaking in this system [27–32]. O_6^+ has also been detected in matrix isolation-infrared experiments [33]. In the present study, we report the first gas phase infrared spectroscopy for O_4^+ and its larger family members O_6^+ and O_8^+ using mass-selected photodissociation.

Early equilibrium mass spectrometry studies of $(O_2)_n^+$ clusters found that dissociation energies for the small species were greater than those expected for electrostatic ion-molecule complexes, raising the possibility of more strongly bound structures with partial covalent bonding [4,5]. For example, the dissociation energy of

$O_4^+ \rightarrow O_2^+ + O_2$ is now generally accepted to be about 10 kcal/mol [4,5,15–18]. Early theoretical studies identified two main structures having stable bonding configurations, the rectangular D_{2h} species and the *trans*-bent C_{2h} species [27]. EPR spectra by Knight et al. for the ions trapped in a neon matrix were assigned to a quartet electronic state of the *trans*-bent species [23]. Jacox and coworkers studied the infrared spectroscopy of O_4^+ , also produced and trapped in a neon matrix [24–26]. The initial assignment of the spectrum was problematic, as there were no theoretical studies and the bands detected were far removed from the vibrations of O_2 ($\omega_e = 1580 \text{ cm}^{-1}$) or O_2^+ ($\omega_e = 1905 \text{ cm}^{-1}$) [34]. However, in a landmark paper, Lindh and Barnes performed extensive computational work on O_4^+ , pointing out the nature of the symmetry breaking in this system and conducting systematic studies to account for the anomalous structures and vibrational frequencies arising from this [29]. The *trans*-bent structure was concluded to be slightly (0.5 kcal/mol) more stable than the rectangular structure, and the computed binding energies of these ions were consistent with the high experimental values. The barrier to rearrangement between these two structures was computed to lie at or just below the dissociation limit. A reanalysis of the IR spectroscopy confirmed that the bands observed were from the asymmetric O–O stretch and its combination with the O–O symmetric stretch, and that these two bands were present for both the rectangular and the *trans*-bent structures [25,29]. Arguments were made to rationalize how the less stable rectangular isomer could be stabilized in the rare gas matrix [25]. In further work on matrices with greater O_2 concentrations, Jacox reported vibrational bands tentatively assigned to O_6^+ [26]. More recent matrix IR work by Andrews and coworkers confirmed the observations of Jacox, and found new spectra attributed to both cyclic and *trans*-bent isomers of O_6^+ [33]. However, there has been no other spectroscopy on larger $(O_2)_n^+$ cluster ions and no gas phase infrared spectroscopy on any of these species.

* Corresponding author. Tel.: +1 706 542 1998; fax: +1 706 542 1234.
E-mail address: maduncan@uga.edu (M.A. Duncan).

In recent work in our lab, we have been able to produce a variety of small molecular ions and their clusters, which we have studied with infrared photodissociation spectroscopy. This work has included metal containing ion-molecule complexes [35–44], carbocations [45–48], and protonated molecular ions [47–52]. In this work, we have found some systems in which isomeric forms are expected but only the single most stable isomer is actually observed [45,51,52]. In other systems, clear evidence is found for a single metastable isomer [47] or for the presence of more than one isomer [46]. The isomeric concentrations in these systems were found to depend on the precursor species employed, the conditions of complex formation, and especially on the details of the molecular potential surface. The O_4^+ system is therefore interesting to examine in the gas phase, where there is no configuration bias from its precursor or surroundings. This system has a relatively high barrier to rearrangement between two possible structures, as well as complex electronic and vibrational structure. As shown below, these factors combine to produce an interesting story for the gas phase spectroscopy of O_4^+ and its larger cluster ions.

2. Experimental

$(O_2)_n^+$ cations are generated with a pulsed nozzle-pulsed electrical discharge cluster source [45–52]. An expansion of pure oxygen or one with oxygen seeded in argon is excited with a pulsed discharge using coaxial ring electrodes. The discharge fires for a 1–2 μ s duration timed in the middle of the 200 μ s gas pulse. The ions produced by this source are cooled by a supersonic expansion and collimated into a molecular beam with a skimmer. These complexes are detected and mass-selected with a reflectron time-of-flight mass spectrometer, as described previously [35,41]. Mass spectra are recorded with a digital oscilloscope (LeCroy “WaveRunner” 6051A) connected to a PC computer via a GPIB interface. Tunable infrared radiation is produced with a specially designed infrared optical parametric oscillator/amplifier (OPO/OPA) system (LaserVision) pumped with a Nd:YAG laser (Spectra Physics PRO-230). The linewidth of the OPO is about 1–2 cm^{-1} and its pulse energy varies from 0.5 to 1.0 mJ/pulse in the lower frequency region (1000–2500 cm^{-1}) of this experiment up to 10 or more mJ/pulse in the higher frequency region 2500–4000 cm^{-1} . Excitation of the mass-selected ions takes place in the turning region of the reflectron, and fragment mass analysis occurs in the flight tube section located after this. Monitoring the yield for one or more fragment ions as a function of frequency generates the infrared spectra.

3. Results and discussion

Fig. 1 shows the mass spectrum of the oxygen cation clusters produced by our discharge source. As shown, the ions produced are those of the form $(O_2)_n^+$. There is no significant concentration of odd-numbered ions such as those which might be produced from oxygen atom or ozone and their clusters with O_2 . Apparently these gentle discharge conditions do not dissociate oxygen efficiently and these ions are not produced. The mass spectrum is optimized for the mass range near O_6^+ , explaining the enhanced abundance of this ion. Under other focusing conditions this ion is not so prominent, and there are also no other ion species that can be identified to have consistently enhanced abundance coming directly from the source.

Fig. 2 shows the photodissociation mass spectra of several of these oxygen cluster ions. In these spectra, the desired cation is mass selected and the mass spectrum is measured with and without the IR photodissociation laser firing. The difference between data accumulated at these two settings produces a mass spectrum with the depletion of the selected parent ion shown as a negative peak and the fragments produced from it as positive peaks. As shown

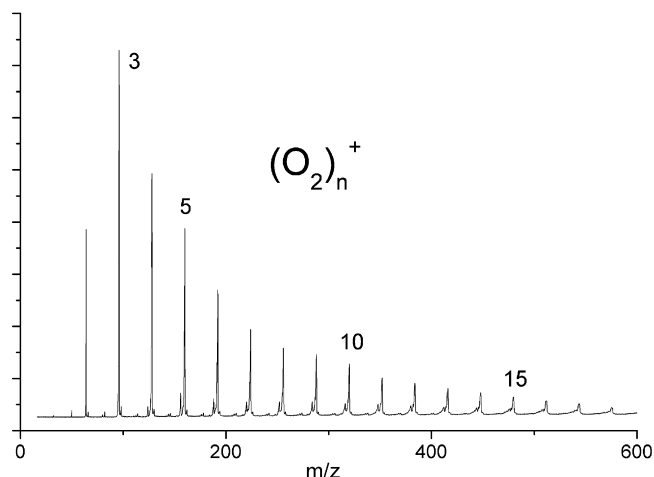


Fig. 1. The mass spectrum of $(O_2)_n^+$ cluster ions produced by the pulsed discharge source.

in the figure, all of these clusters fragment by eliminating one or more intact O_2 molecules. The photon energy for these dissociation experiments is set at 2840 cm^{-1} , where O_4^+ and all the other ions absorb on a broad continuum (see below). All of these larger cluster ions are found to have at least some absorption/fragmentation intensity at this photon energy. Therefore, the dissociation energies for all of these ions can be concluded to lie below 2840 cm^{-1} or about 8.12 kcal/mol. Table 1 shows the dissociation energies that have been determined previously for $(O_2)_n^+$ ions, for $n=2-8$. As shown, this upper limit for the dissociation energy is consistent with the values determined previously for the $n=3-8$ clusters, but is a little lower than the threshold determined before for O_4^+ . More

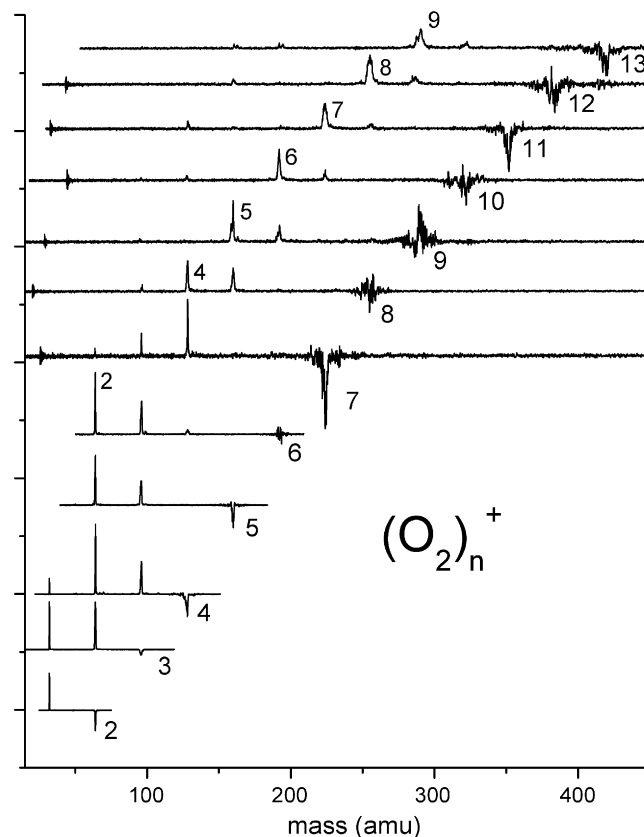


Fig. 2. The photodissociation mass spectra of $(O_2)_n^+$ clusters for various values of n .

Table 1

The dissociation energies (kcal/mol) for $(\text{O}_2)_n^+ \rightarrow (\text{O}_2)_{n-1}^+ + \text{O}_2$ determined by different research groups.

Cluster size, n	CJ ^a	LON ^b	H ^c	MPSSM ^d
2	10.53	9.69	9.15	
3	6.51		5.89	
4	2.56		2.48	
5	2.43		2.14	3.69
6	2.0		1.92	
7			1.89	2.54
8			1.85	2.54

^a Conway and Janick [15].

^b Linn, Ono and Ng [16].

^c Hiraoka [17].

^d Matt, Parajuli, Stamtoric, Sheier, and Märk [18].

exact information on the dissociation limits for the $n=2-4$ ions is obtained from the tunable IR spectra presented below. The larger cluster ions in Fig. 2 fragment by losing more than one O_2 unit. Beginning at the $n=9$ species and continuing up to the $n=12$ cluster, all of these lose four O_2 units, indicating an upper limit on the average binding energy of roughly $2840/4 = 710 \text{ cm}^{-1}$ (2.03 kcal/mol) for these larger clusters. The dissociation energies determined previously for the larger clusters are all just below 2.0 kcal/mol, and therefore these IR dissociation processes are consistent with the energetics derived previously.

Fig. 3 shows the IR photodissociation spectrum measured in two different ways for the O_4^+ ion. In the upper trace, “neat” O_4^+ is mass selected and excited with the IR laser, and sharp bands are detected in the O_2 elimination channel beginning at about 2900 cm^{-1} . However, no other efficient photodissociation signal is detected at lower energies by this dissociation method. In particular, we do not detect any strong signal near the 1164 or 1320 cm^{-1} bands reported in IR absorption by Jacox [24]. However, this is understandable, because of the photodissociation method employed here. At the low laser

powers available with our OPO system, we do not usually see efficient photofragmentation unless we are above the one-photon dissociation threshold. The dissociation energy of O_4^+ has been reported previously to lie at $9-10 \text{ kcal/mol}$ ($3150-3500 \text{ cm}^{-1}$), and so we do not expect to be able to detect photodissociation at energies below this. In fact, the first sharp band in the photodissociation signal begins at just under 2900 cm^{-1} , and this is slightly lower in energy than the previously reported dissociation threshold. Because of this observation, we can revise the dissociation energy of O_4^+ downward to be $\leq 2900 \text{ cm}^{-1}$ (8.3 kcal/mol). It is also noticeable that there is an underlying continuum of dissociation signal in this spectrum that begins at roughly 2600 cm^{-1} . It is likely that this signal represents direct absorption into the dissociation continuum. If this is true, then the dissociation threshold would be even lower, i.e., $2600 \text{ cm}^{-1} = 7.4 \text{ kcal/mol}$. However, it is important to note that both of these apparent dissociation limits could be lower than the actual dissociation energy if the molecule contains internal energy from the cluster growth or plasma conditions. Based on past experience with other similar systems studied in our instrument, we do not expect ions this small to have significant amounts of internal energy, and therefore we believe these dissociation limits to be valid.

Although it is not a strong signal, there is some broad, weak structure in the $800-1400 \text{ cm}^{-1}$ region, enhanced in the inset box of the figure. This structure occurs well below the anticipated dissociation limit for this ion, and therefore it should not be possible to detect photofragmentation here. This signal could be produced from a small concentration of ions that were not cooled effectively by the cluster source and retain some residual internal energy. This unquenched energy can add to that of the IR photon to accomplish fragmentation below the one-photon dissociation threshold. Another possible mechanism for dissociation here is $1+1$ resonance-enhanced two-photon absorption. This is possible because this energy region is about halfway to the dissociation threshold. A combination of these processes may also be at work here, but in any event this signal is so weak that it clearly does not correspond to one-photon dissociation. Its broad structure also cannot be interpreted as meaningful, because of the complex mechanism likely involved. Resonant $1+1$ absorption may also be involved in the broad feature at 2767 cm^{-1} .

The second spectrum in Fig. 3 is that for the O_4^+ ion “tagged” with argon. The method of “spectator” atom attachment or “tagging” is now well known in infrared photodissociation spectroscopy [35,53–56]. IR photons in the region of vibrational fundamentals are not usually energetic enough to break bonds directly, and so attachment of a weakly bound tag atom often can be used to increase the dissociation yield without significantly perturbing the spectrum. Because the tag atom is weakly bound to the system, cold complexes are preferentially sampled by this method. The actual degree of perturbation induced by the tag atom is always a question, but this can be addressed by theory on the ion with and without the tag or by measuring the spectrum both ways, if possible. Because theory on O_4^+ itself is so difficult, we have not tried to do computational studies on $\text{O}_4^+ \text{Ar}$. However, as shown in Fig. 3, the higher frequency region of the O_4^+ spectrum, where we are apparently above the dissociation limit, is reproduced almost exactly in the argon tagged spectrum. The band positions in the two spectra are the same within $1-2 \text{ cm}^{-1}$ for many of the sharp features in the 3000 cm^{-1} region. It is therefore a safe assumption that the argon tag atom used here does not induce a significant perturbation on the system. The tagged spectrum can therefore be trusted to faithfully reproduce the spectrum in the lower energy region below the dissociation threshold of O_4^+ , where no efficient dissociation can be detected without the tag. As shown, a strong band is observed here for $\text{O}_4^+ \text{Ar}$ at 1323 cm^{-1} , but there are no other bands detected in the spectral range investigated (down to 700 cm^{-1}). The high efficiency

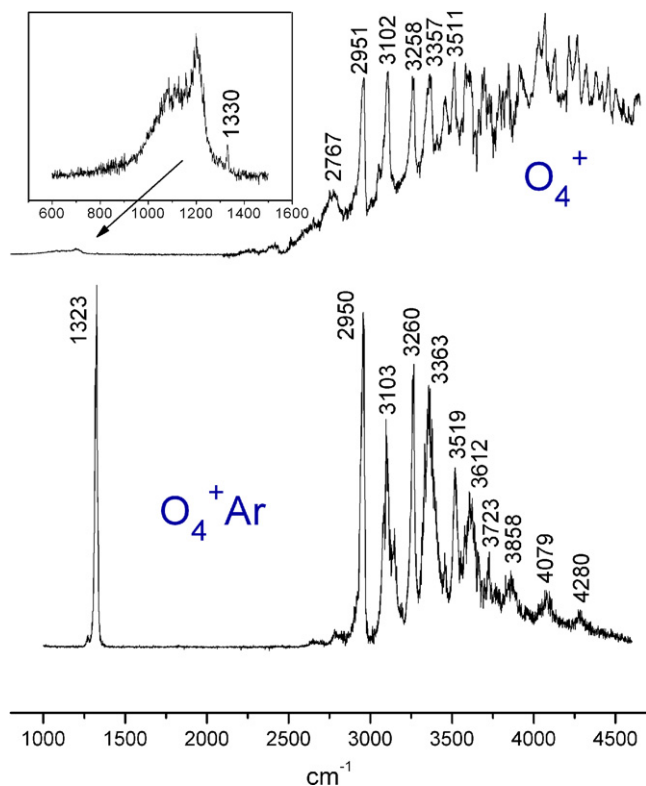


Fig. 3. The infrared photodissociation spectra of O_4^+ and $\text{O}_4^+ \text{Ar}$.

Table 2
The vibrational bands observed for $\text{O}_4^+/\text{O}_4^+\text{Ar}$, $\text{O}_6^+/\text{O}_6^+\text{Ar}$ and O_8^+ with their assignments.

Band position	Frequency combinations	Assignment
$\text{O}_4^+/\text{O}_4^+\text{Ar}$		
–/1323	1323	ν_5 (asym. O—O stretch)
2760/–	1323 + 1437	$\nu_5 + ?$
2951/2950	1323 + 1627	$\nu_5 + \nu_1$ (sym. O—O stretch)
3102/3103	1323 + 1627 + 153	$\nu_5 + \nu_1 + \nu_4$ (torsion)
3258/3260	1323 + 1627 + 310	$\nu_5 + \nu_1 + \nu_3$ (sym. in-plane bend)
3357/3363	1323 + 1627 + 153 + 260	$\nu_5 + \nu_1 + \nu_4 + \nu_2$ (O_2 — O_2 stretch)
3456/3458	1323 + 1627 + 260 + 248	$\nu_5 + \nu_1 + 2\nu_2$
3511/3519	1323 + 1627 + 310 + 249	$\nu_5 + \nu_1 + \nu_3 + \nu_2$
–/3612	1323 + 1627 + 153 + 260 + 249	$\nu_5 + \nu_1 + \nu_4 + 2\nu_2$
–/3723	1323 + 1627 + 2(310) + 153	$\nu_5 + \nu_1 + 2\nu_3 + \nu_4$
–/3858	1323 + 1627 + 153 + 260 + 249 + 246	$\nu_5 + \nu_1 + \nu_4 + 3\nu_2$
–/4079	1323 + 1627 + 153 + 260 + 249 + 246 + 221	$\nu_5 + \nu_1 + \nu_4 + 4\nu_2$
–/4280	1323 + 1627 + 153 + 260 + 249 + 246 + 221 + 201	$\nu_5 + \nu_1 + \nu_4 + 5\nu_2$
$\text{O}_6^+/\text{O}_6^+\text{Ar}$		
1335/–	1335	Asym. O—O stretch
1413/1425	1425	Asym. O—O stretch
2841/2846	1425 + 1421 (or 1335 + 1506)	Asym. O—O stretch $2\times$
3036/3038	1425 + 1613	Asym. + sym. O—O stretch
O_8^+		
1426	1426	ν_a (asym. O—O stretch)
1488	1488	ν_b (asym. O—O stretch)
2865	1426 + 1439 or 1488 + 1377	$\nu_a + 1439$ or $\nu_b + 1377$
2916	1426 + 1490	$\nu_a + \nu_b$
3025	1426 + 1599	$\nu_a + \text{free O}_2$

of the photodissociation at this 1323 cm^{-1} band suggests that the argon binding energy is well below this energy. The weak, broad signal detected for neat O_4^+ near 1000 – 1300 cm^{-1} is not detected here, and can be ruled out from further consideration.

We can compare these gas phase photodissociation spectra to the infrared absorption spectrum measured by Jacox for the O_4^+ ion isolated in a neon matrix [24,25]. As noted above, the assignment of the spectrum observed by Jacox was initially questionable because the main bands were at much lower frequencies than those for either O_2^+ or O_2 [24]. However, after the theoretical work by Lindh and Barnes [29], the spectral assignment became clear [25]. The delocalized charge in the O_4^+ system gave rise to the unusually low frequencies. Bands at 1164 and 2809 cm^{-1} were assigned to the *trans*-bent structure and another set of bands at 1320 and 2949 cm^{-1} were assigned to the rectangular isomer. Additional signals were detected above 3000 cm^{-1} , but this region was partially obscured by absorption from CO_2 present in that experiment and a background impurity of water (Marilyn Jacox, private communication). Our spectrum has no strong signal near the Jacox bands assigned to the *trans*-bent isomer, but our bands at 1323 and 2950 cm^{-1} are remarkably close to those seen in the matrix spectrum at 1320 and 2949 cm^{-1} . We therefore assign our bands at these positions in the same way that Jacox did, i.e., to the rectangular isomer. The 1323 cm^{-1} band is then the O—O asymmetric stretch (ν_5) and the 2950 cm^{-1} band is the combination of this asymmetric O—O stretch with the symmetric O—O stretch, i.e., $\nu_5 + \nu_1$. The ν_1 O—O stretch symmetric stretch is therefore inferred to have a frequency of about 1627 cm^{-1} . This region of the spectrum and its comparison to the Jacox spectra [24,25] and to the theory of Lindh and Barnes [29] indicates that our experiment produces primarily the rectangular isomer and not the *trans*-bent species. We cannot rule out the presence of a small amount of the *trans*-bent species lying below our sensitivity. A weak broad feature seen in the tagged spectrum at about 2785 cm^{-1} is the closest thing to the expected 2809 cm^{-1} band, but there is nothing near the expected 1164 cm^{-1} band. We therefore conclude that the concentration, if any, for the *trans*-bent species must be considerably less than that for the rectangular species.

As shown in Fig. 3, the region of the spectrum above 3000 cm^{-1} contains a series of closely-spaced bands that appear in both the neat and the tagged spectra for O_4^+ . In the tagged spectrum, some of the bands are sharper than others, and there is less of the continuum signal that underlies the bands in the neat spectrum. The first several bands in this region fall at essentially the same positions in both spectra. However, the bands at higher energy become broader and less well-defined in the neat spectrum, making it difficult to identify the common features in both spectra. We therefore focus our discussion primarily on the bands in the tagged spectrum, which are more cleanly resolved. The bands in this region were not reported in the previous work by Jacox (private communication). However, Jacox has communicated to us that an unassigned line was seen in that data at 3254 cm^{-1} (Marilyn Jacox, private communication), which compares quite nicely with the band that we see at 3258 or 3260 cm^{-1} in the neat and tagged spectra respectively. Apparently, the matrix data detects this one feature common to our spectrum and others that we see here were either too weak to be detected or overlapped with other signals.

Vibrational fundamental bands for O_4^+ are not expected in this high frequency region of the spectrum for either isomer of O_4^+ because all of the computed vibrational frequencies occur in the region below 1500 cm^{-1} [29]. This led to some of the initial confusion in the assignment of the IR spectrum observed by Jacox. However, the bands in the matrix spectrum at 2809 and 2948 cm^{-1} were assigned convincingly to combination bands involving one quanta each of the asymmetric and symmetric O—O stretches for the two isomers, respectively. These two vibrations are the only ones expected to arise from a two-mode combination for either isomer of O_4^+ . Therefore, the bands at frequencies higher than the 2950 cm^{-1} feature must arise from multi-mode combinations involving low frequency modes for the rectangular species. There are several low frequency stretches, torsions and bends expected in this system (see below). We therefore have made our best attempt to assign these bands with the fewest number of vibrational combinations possible. Additionally, we note that there is a sharp/broad alternation in the lines in the tagged spectrum. For example, the bands at

2950, 3260 and 3519 cm^{-1} are noticeably sharper than others in this region. The different linewidths may be associated with the different rotational contours expected for different band types (parallel versus perpendicular). Another possibility is that the predissociation rates in this region of the spectrum are vibration-specific. In either scenario, the sharp versus broad line groups should have some connections, and we take this into account in our assignments.

Table 2 provides a list of all the vibrational bands measured for O_4^+ (as well as those for O_6^+ and O_8^+ discussed below) and their possible assignments. As indicated, there are far too many bands to be assigned to “simple” one-quanta combinations of different vibrations. Instead, it appears that there must be multiple quanta progressions in certain frequencies. For example, the series of broad bands at 3103, 3363, 3612, 3858, 4079 and 4280 cm^{-1} are spaced by 260, 249, 246, 221 and 201 cm^{-1} , suggesting a progression in the initial 260 cm^{-1} frequency with anharmonicity reducing the spacings toward the higher members of the series. Although the series is not exactly regular as reflected in these band positions, the bands are broad and noisy and our uncertainty in their center positions is roughly $\pm 5 \text{ cm}^{-1}$ at the lower energies and worse than this for the weaker high energy bands. As shown in the table, this 260 cm^{-1} frequency and multiple-quanta progressions of it, as well as two other intervals of 310 and 153 cm^{-1} , are enough to account for virtually all the bands in the spectrum.

Table 3 shows the vibrational frequencies computed by Lindh and Barnes for the different vibrations of O_4^+ in the rectangular structure [29]. As discussed in their paper, the frequencies of these vibrations varied considerably with different levels of theory. The asymmetric O–O stretch vibration (ν_5) was especially problematic because of the symmetry breaking in this system, and heroic methods were required to derive the frequency recommended for this mode. However, as discussed by Jacox [25], it is then possible to identify the fundamental of this vibration at 1323 cm^{-1} . As noted above, the band at 2950 cm^{-1} is the combination of the asymmetric O–O stretch (ν_5) with the O–O symmetric stretch (ν_1), and the latter frequency is then 1627 cm^{-1} . Using the higher frequency bands, we have repeated occurrences of the intervals 310, 260 and 153 cm^{-1} . The computed frequencies of the lower frequency vibrational modes are distinctive enough to allow us to identify these with the ν_3 (symmetric in-plane bend), ν_2 (O_2 – O_2 stretch) and ν_4 (torsion) vibrations, respectively. We therefore have identified five out of the six vibrations for O_4^+ . Using the combination band intervals to assign fundamental frequencies assumes that there is no significant off-diagonal anharmonicity in these modes, but this is the best assignment that can be made at this time. As shown in the table, the experimental and computed frequencies are not in perfect agreement, but the comparison is rather good considering the complexity of this system for theory. Because we do not see the bands expected at 1164 and 2809 cm^{-1} for the *trans*-bent species, and because all the bands in our spectrum can be assigned to frequencies near those computed for the rectangular D_{2h} structure, we conclude again that this is the only isomer present.

It is interesting to consider why so many combination bands are detected for this O_4^+ species, and also why their IR activity is

focused in the 2950–4000 cm^{-1} region. This weakly bound species has complex molecular structure, and it was noted by Lindh and Barnes from their calculations that the charge distribution about this molecule varies dramatically with small molecular displacements [29]. The dipole derivatives which give rise to IR intensities are therefore unusually high. Although some combination bands were reported in the previous absorption spectroscopy, it is important to emphasize that we are measuring photodissociation spectra here. The energy region above 3000 cm^{-1} is above the dissociation threshold for O_4^+ . Therefore, the bands that we detect are the result of vibrational predissociation, and the dissociation yield may be strongly enhanced in this region beyond the absorption intensity. This could explain why we see bands that were not detected in the matrix absorption spectra. It is then also reasonable that certain vibrations might be more effective in dissociation (i.e., have an enhanced rate), perhaps explaining the occurrence of the broad versus sharp vibrational bands. In particular, it can be seen from the vibrational assignments in Tables 2 and 3 that the 260 cm^{-1} vibration is the O_2 – O_2 stretch, which is the dissociation coordinate. It is therefore completely reasonable that excitation of this vibration, especially in multiple quanta, would give rise to efficient dissociation, and broader linewidths. What is actually remarkable is that these O_2 – O_2 stretch vibrational bands can be detected above the dissociation limit, even at energies up to 1000 cm^{-1} beyond the threshold. However, because these bands are combinations with the asymmetric and symmetric O–O stretches, most of the vibrational energy is not in the dissociation coordinate. Apparently, when the O_2 – O_2 stretch occurs in combination with other vibrations, the direct dissociation is inhibited enough to allow a finite lifetime for these levels. However, these broad bands do have one or more quanta in the O_2 – O_2 stretch, and this apparently makes their predissociation rates greater than those for the other sharper bands in this same energy range that do not have this vibration excited. Although it is not clear at all that these bands are homogeneously broadened, the linewidth of the 3363 cm^{-1} band, for example, which is about 70 cm^{-1} , would correspond to a predissociation lifetime of about 70 fs. Interestingly, Johnson and coworkers also detected multiplet band structure near 4000 cm^{-1} for the O_4^- anion, which they assigned to an electronic transition with vibronic progressions [57].

It is interesting that the spectroscopy of O_4^+ here indicates the presence of only the D_{2h} rectangular isomer and that the C_{2h} *trans*-bent species is not detected at all. The *trans*-bent species is actually computed to be slightly more stable than the rectangular species [29]. In the gas phase plasma of our source, it should be possible for cluster growth to sample the geometrical configurations necessary to produce either of these species. In our previous studies on hydrocarbon ions, we have seen biases for the production of certain isomers because of the structure of the precursors employed [46]. However, it is not clear how such a bias could arise for the clustering of O_2 species. There is also no obvious bias in the detection scheme that should selectively sample only the rectangular species; both have similar IR transition strengths and dissociation energies [24,25,29]. Our conclusion is therefore that the gas phase environment only produces the rectangular species, even though the matrix environment produced both isomers. It is conceivable that the neon matrix environment could produce the *trans*-bent isomer and stabilize it preferentially. Mobility through the matrix is required for cluster growth, but if the *trans*-bent species is formed initially via end-on contact, rotational or torsional motions that might be required to rearrange to the rectangular structure could be hindered in this environment and the activation energy required is not available. The gas phase environment does not have the configuration bias of the matrix, and ions grow at warmer temperatures, therefore making it more likely to produce the more stable species. We conclude therefore that the rectangular structure of O_4^+ is actually

Table 3
The vibrational frequencies for O_4^+ and their comparison to theory [29].

Vibration	Assignment	Present experiment	Theory
ν_1	Symmetric O–O stretch	1627	1680–1710
ν_2	O_2 – O_2 stretch	260	249–250
ν_3	Sym. in-plane bend	310	379–380
ν_4	Torsion	153	176
ν_5	Asym. O–O stretch	1323	1271
ν_6	Asym. in-plane bend	–	40–60

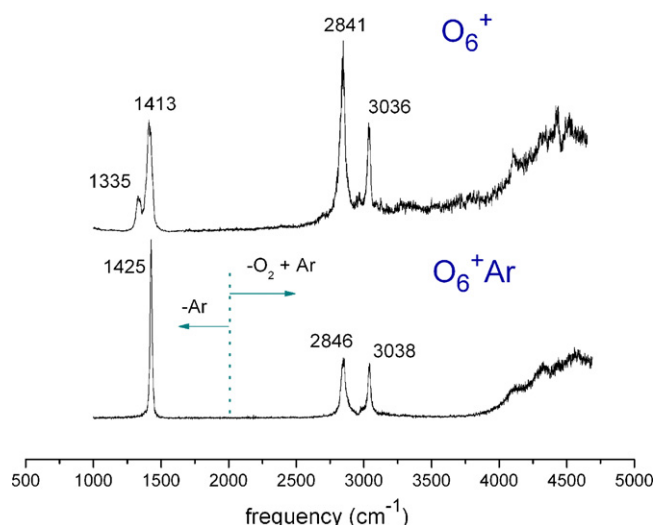


Fig. 4. The infrared photodissociation spectra of O_6^+ and O_6^+Ar .

the most stable structure for this ion. This contradicts the accepted computational work on this ion, which finds the *trans*-bent species to be slightly more stable (by 0.5 kcal/mol) [29]. However, considering the complexity of the electronic structure of this ion, an error in the relative stability of these isomers is perhaps understandable. Additional computational work could investigate this issue in the future.

Fig. 4 shows the IR photodissociation spectrum for the O_6^+ ion measured “neat” by the elimination of O_2 and “tagged” by the elimination of argon. In the tagged spectrum, the fragmentation channel at higher energy is actually the loss of both argon and O_2 , while at lower energy it is the loss of argon only. The band positions measured in both spectra are listed in Table 2. Somewhat broad features are detected in the neat spectrum at 1335, 1413, 2841 and 3036 cm^{-1} . In the low energy section of the tagged spectrum, the 1335/1413 doublet seen for neat O_6^+ is replaced by a single sharp band at 1425 cm^{-1} for the tagged ion, and the two higher energy bands have nearly the same positions at 2846 and 3038 cm^{-1} for both the neat and the tagged species. The high efficiency of the photodissociation at the 1425 cm^{-1} band suggests that the argon binding energy is well below this energy. The dissociation energy of the neat complex was determined previously to be 5.89 kcal/mol [17], and so one-photon dissociation should not be possible for this species below 2060 cm^{-1} . The bands in the neat spectrum at 1335 and 1413 cm^{-1} must therefore be the result of either hot-band absorption, as discussed earlier, or 1 + 1 resonance-enhanced two-photon absorption. The latter seems possible for either band because both are more than halfway in energy to the dissociation threshold. However, the disappearance of the 1335 cm^{-1} band in the tagged spectrum suggests that this was the result of absorption by internally hot molecules. The significant shift in the 1413 band to 1425 cm^{-1} also suggests this. We therefore focus primarily on the assignment of the tagged spectrum, which should represent the cold molecules.

The first feature in the spectrum at low energy is the sharp and intense band at 1425 cm^{-1} . By analogy to the spectrum discussed above for O_4^+ , this is likely an IR-active asymmetric O–O stretching vibration. Like the corresponding band in the O_4^+ spectrum, this band occurs at a frequency lower than those for either the neutral O_2 molecule or the O_2^+ diatomic ion. We therefore conclude that it is likely an asymmetric O–O stretch in an ion with a charge delocalized over more than one O_2 moiety, like the O_4^+ species. The two higher frequency

bands here likely arise from combinations of the 1425 vibration with other relatively high frequency vibrations. As in the case of O_4^+ , no high frequency fundamentals are expected in the 2800–3000 cm^{-1} for clusters involving only oxygen molecules. The 2846 cm^{-1} band lies at almost exactly twice the frequency of the 1425 cm^{-1} band (1425 + 1421), consistent with an overtone of the lower frequency vibration. The 3038 cm^{-1} band occurs at a frequency of 1425 + 1613 cm^{-1} , implying that there is a symmetric O–O stretch at this frequency like that seen at 1627 cm^{-1} for O_4^+ .

The most telling band in the O_6^+ spectrum is the one at 1425 cm^{-1} . Although this is in roughly the same region as the corresponding feature at 1323 cm^{-1} for O_4^+ , its frequency is about 100 cm^{-1} different from that for the O_4^+ band. This indicates that O_6^+ is not simply an O_2 -solvated O_4^+ species, but instead has a distinctly different ionic structure. Consistent with this, the dissociation energy for O_6^+ is lower than that for O_4^+ , but it is not as low as the value for the larger clusters here (about 2 kcal/mol [17]). Moreover, the frequency of the O_6^+ ion is significantly higher than that in O_4^+ . This could indicate a more strongly bound species, but the dissociation energy of O_6^+ is considerably less than that of O_4^+ . A higher frequency could also result if the charge is somewhat more localized on one O_2 unit, thus approximating the frequency of the O_2^+ diatomic cation ($\omega = 1905 cm^{-1}$). Another possibility is that the O_2 moieties in the O_6^+ structure are confined geometrically in a configuration in which their vibrational motion is more hindered. Depending on the structure, the increased repulsion at the outer turning point of a hindered vibration can cause an increase in frequency compared to a vibration whose motion is into free space [35,36,41]. An intriguing possibility is that O_6^+ is cyclic, built on the binding motif of the planar *cis*-bent configuration suggested previously to be stable for O_4^+ [29]. Such a cyclic structure could explain the higher vibrational frequency, but a *trans*-bent structure might also be consistent with this. A cyclic O_6^+ structure is also an attractive explanation for the spectrum because of its high symmetry. We see only one IR-active O–O stretching band in the spectrum, which suggests a high-symmetry structure. Computational treatments of O_6^+ , which could provide further insight into structural issues, are likely to have the same symmetry-breaking issues seen for O_4^+ and are thus beyond the scope of this study. However, the frequencies measured here will hopefully provide incentive for future computational studies on this ion.

In previous work on O_6^+ , Andrews and coworkers found infrared bands at 1435.0 and 1429.5 cm^{-1} in a neon matrix that they assigned to cyclic and *trans*-bent isomers, respectively [33]. These assignments were based on the frequency shifts resulting from partially resolved spectra measured with isotopic substitutions and on the predictions of preliminary density functional theory computations. Experiments in an argon matrix found only one band at 1416.1 cm^{-1} , which was attributed to the cyclic species. Because of its prominence in the argon experiment, where structural rearrangements occur more readily, the cyclic isomer was concluded to be the most stable. Our gas phase spectrum also has only one peak in this region, and is thus likely to arise from the most stable isomer of O_6^+ . However, if we assume that the neon matrix shifts for this ion are similar to those seen for O_4^+ , our 1425 cm^{-1} band seems to agree best with the matrix band at 1429.5 cm^{-1} , which Andrews assigned to the *trans*-bent species. According to Andrews, though, this is the band that dropped out in the argon experiments. It seems therefore that there is still some considerable uncertainty about which matrix bands correspond to which isomer, and also which of these correspond to the single band in this region seen in the gas phase spectrum. Again, new theoretical work is needed to elucidate these issues.

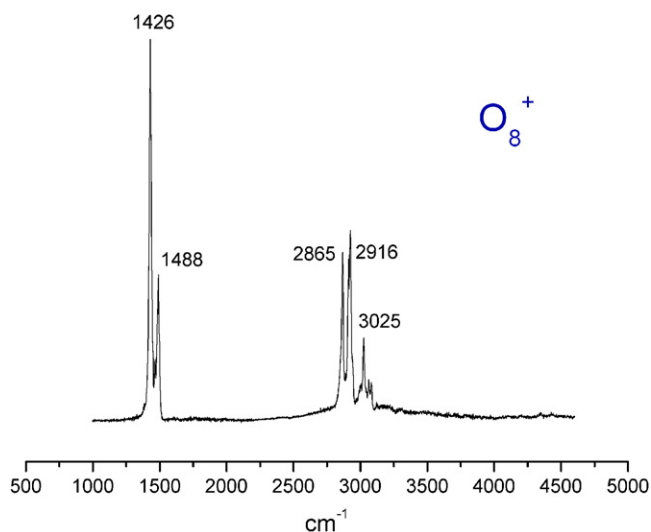


Fig. 5. The infrared photodissociation spectrum of O_8^+ .

Fig. 5 shows the IR photodissociation spectrum measured for the O_8^+ cation in the O_2 elimination channel. The dissociation energy of O_8^+ is 2.5 kcal/mol [17] and therefore photodissociation should be possible above about 870 cm^{-1} . As shown, the bands in the spectrum all lie above this, and the dissociation is efficient. In the higher energy region, the spectrum can also be measured in the channel corresponding to the loss of two O_2 molecules. This spectrum is the same as that shown, except that it has the underlying continuum signal seen above for O_4^+ and O_6^+ . Therefore, we did not employ argon tagging for this system. Five sharp bands are detected in the spectrum at 1426, 1488, 2865, 2916 and 3025 cm^{-1} . These bands fall in the same two general regions of the spectrum seen already for the O_4^+ and O_6^+ ions. Using the same logic applied before, we therefore expect that the 1426 and 1488 cm^{-1} bands represent asymmetric O–O stretch vibrations, while the higher frequency bands represent combinations of lower frequencies. Table 2 shows the frequency intervals for the combinations.

Two features of these bands are especially revealing about the likely structure of O_8^+ . First of all, the 1426 cm^{-1} band falls at almost exactly the same frequency as the single strong band seen at 1425 cm^{-1} for O_6^+ . Secondly, the 3025 cm^{-1} band falls at a combined frequency of 1426 + 1599 cm^{-1} or else it is 1488 + 1537 cm^{-1} . Either of the 1599 or 1537 cm^{-1} intervals is higher than any of the single-quanta frequencies assigned for O_4^+ or O_6^+ and these are remarkably close to the frequency of the free neutral O_2 molecule ($\omega_e = 1580$ cm^{-1} ; fundamental = 1566 cm^{-1}). Small polarization of a neutral O_2 is likely to remove antibonding character from the highest occupied $2p^*$ orbital, thus increasing the frequency slightly (complete removal of an electron in the case of O_2^+ causes the frequency to shift to $\omega_e = 1905$ cm^{-1}). Thus, if the cluster had an attached neutral O_2 , it would likely have a slightly higher frequency than usual, consistent with the 1599 cm^{-1} value. Both the observation of the 1426 cm^{-1} band and the 1599 cm^{-1} combination interval suggest that O_8^+ is best described as an O_2 -solvated O_6^+ ion. The observation of the 1488 band, which is weaker than but close to the 1426 band, is consistent with a slight symmetry breaking in the O_6^+ core ion by an attached O_2 , which also fits into this scenario. Also consistent with this is the dissociation energy for O_8^+ . The value of 2.5 kcal/mol is only slightly greater than those for the largest clusters studied here (converged at large n to about 2 kcal/mol) [17]. The spectroscopy and dissociation energies agree that O_8^+ is a solvated O_6^+ , and we expect that the same would be true for the still-larger $(O_2)_n^+$ clusters.

4. Conclusion

Cluster cations of oxygen, i.e., $(O_2)_n^+$, produced with a pulsed supersonic discharge source, have been studied with mass-selected infrared photodissociation spectroscopy. The dissociation energies of the various $(O_2)_n^+$ ions measured with infrared excitation are compared to those measured previously with collision induced dissociation. The threshold for the O_4^+ ion was found to be slightly lower than the former value, but otherwise the present values agree well with those determined previously. The dissociation energies for O_4^+ and O_6^+ are both higher than those for the other clusters, consistent with partial covalent character in these systems rather than simple electrostatic interactions.

Infrared spectra were measured for the O_4^+ , O_6^+ and O_8^+ species over the range of about 800–4000 cm^{-1} . O_4^+ is found to have resonances assigned previously to a rectangular D_{2h} structure in neon matrix experiments. The gas phase frequencies are within a few cm^{-1} of the neon matrix values, allowing a nice comparison of these two experiments. The *trans*-bent C_{2h} structure reported previously to be slightly more stable than the rectangular isomer, and seen in matrix isolation spectroscopy, was not detected in these gas phase experiments. The production of the *trans*-bent isomer in neon matrices is suggested to arise from steric constraints of growth and rearrangement in that solid environment. The gas phase growth in the present experiment, where significant energy and no steric constraints are present, apparently allows this ion to find its most stable structure. Interestingly, Johnson and coworkers have recently reported a study similar to ours for the O_4^- anion, which is also concluded to have a rectangular structure (see Ref. [57] and accompanying paper in the present journal). O_4^+ has unusual vibrational activity in a number of combination bands lying in the energy range at and just above the dissociation energy for this ion. Broader linewidths are observed for those vibrational bands having activity in the O_2 – O_2 stretch vibration, indicating enhanced predissociation for this mode. This is not surprising, as this vibration is the dissociation coordinate. Combination band intervals for this system allow five out of the expected six vibrational frequencies to be determined, and these values are in good agreement with the predictions of theory.

The O_6^+ cation is found to have a distinctly different vibrational spectrum from O_4^+ , indicating that it is not simply an O_2 -solvated O_4^+ ion, but rather has its own characteristic structure. We suggest that a cyclic structure fits all the circumstantial evidence, but comparisons to previous matrix isolation spectra raise questions about this. Careful computational studies are needed to assign the spectrum reliably and to decide what the structure is. O_8^+ on the other hand, has vibrational features suggesting that it is an O_2 -solvated O_6^+ ion. Some of its vibrations occur at almost the same frequencies as those of O_6^+ and other features are consistent with slight symmetry breaking in O_6^+ induced by an additional O_2 . Larger clusters are presumed to have a similar structural trend. All of these oxygen ion clusters have fascinating molecular properties that are revealed by these IR studies.

Acknowledgements

We acknowledge generous support for this work from the Air Force Office of Scientific Research (grant no. FA9550-06-1-0028) and the National Science Foundation (grant no. CHE-0551202).

References

- [1] G.R. Reid, Adv. Atom. Mol. Phys. 12 (1976) 375.
- [2] E.E. Ferguson, F.C. Fehsenfeld, D.L. Albritton, Gas Phase Ion Chemistry, vol. 1, Academic Press, New York, 1979, p. 45.
- [3] F. Arnold, A.A. Viggiano, Planet. Space Sci. 30 (1982) 1295.
- [4] J.-H. Yang, D.C. Conway, J. Chem. Phys. 40 (1964) 1729.

- [5] D.C. Conway, J.-H. Yang, *J. Chem. Phys.* 43 (1965) 2900.
- [6] I.C. Plumb, D. Smith, N.G. Adams, *J. Phys. B: Atom. Mol. Phys.* 5 (1972) 1762.
- [7] R.N. Varney, M. Pahl, T.D. Märk, *Acta Phys. Aust.* 38 (1973) 287.
- [8] V. Nestler, P. Warneck, *Chem. Phys. Lett.* 45 (1977) 96.
- [9] M.J. Weiss, J. Berkowitz, E.H. Appelman, *J. Chem. Phys.* 66 (1977) 2049.
- [10] I. Dotan, J.A. Davidson, F.C. Fehsenfeld, D.L. Albritton, *J. Geophys. Res.* 83 (1978) 4036.
- [11] A.B. Raksit, *Int. J. Mass Spectrom. Ion Processes* 69 (1986) 45.
- [12] J.L. Dulane, M.A. Biondi, R. Johnsen, *Phys. Rev. A: Atom. Mol. Opt. Phys.* 37 (1988) 2539.
- [13] N. Gee, G.R. Freeman, *Radiat. Phys. Chem.* 32 (1988) 59.
- [14] F. Cacace, G. de Petris, M. Rosi, A. Troiani, *Chem. Eur. J.* 8 (2002) 3653.
- [15] D.C. Conway, G.S. Janik, *J. Chem. Phys.* 53 (1970) 1859.
- [16] S.H. Linn, Y. Ono, C.Y. Ng, *J. Chem. Phys.* 74 (1981) 3348.
- [17] K. Hiraoka, *J. Chem. Phys.* 89 (1988) 3190.
- [18] S. Matt, R. Parajuli, A. Stamatovic, P. Scheier, T.D. Mark, *J. Chem. Phys.* 116 (2002) 7583.
- [19] R.A. Beyer, J.A. Vanderhoff, *J. Chem. Phys.* 65 (1976) 2313.
- [20] M.L. Vestal, G.H. Mauclaire, *J. Chem. Phys.* 67 (1977) 3767.
- [21] G.P. Smith, P.C. Cosby, J.T. Moseley, *J. Chem. Phys.* 67 (1977) 3818.
- [22] G.P. Smith, L.C. Lee, *J. Chem. Phys.* 69 (1978) 5393.
- [23] L.B. Knight Jr., S.T. Coblanchi, J. Petty, *J. Chem. Phys.* 91 (1989) 4423.
- [24] W.E. Thompson, M.E. Jacox, *J. Chem. Phys.* 91 (1989) 3826.
- [25] M.E. Jacox, W.E. Thompson, *J. Chem. Phys.* 100 (1994) 750.
- [26] C.L. Lugez, W.E. Thompson, M.E. Jacox, *J. Chem. Phys.* 105 (1996) 2153.
- [27] J.B. Peel, *J. Chem. Phys.* 94 (1991) 5774.
- [28] J.B. Peel, *Chem. Phys. Lett.* 218 (1994) 367.
- [29] R. Lindh, L.A. Barnes, *J. Chem. Phys.* 100 (1994) 224.
- [30] L.A. Barnes, R. Lindh, *Chem. Phys. Lett.* 223 (1994) 207.
- [31] C.D. Sherrill, A.I. Krylov, E.F.C. Byrd, M. Head-Gordon, *J. Chem. Phys.* 109 (1998) 4171.
- [32] C.D. Sherrill, M.S. Lee, M. Head-Gordon, *Chem. Phys. Lett.* 302 (1999) 425.
- [33] M. Zhou, J. Hacialoglu, L. Andrews, *J. Chem. Phys.* 110 (1999) 9450.
- [34] K.P. Huber, G. Herzberg, *Molecular Spectra and Molecular Structure. IV. Constants of Diatomic Molecules*, Van Nostrand Reinhold, New York, 1979.
- [35] M.A. Duncan, *Int. Rev. Phys. Chem.* 22 (2003) 407.
- [36] N.R. Walker, G.A. Grieves, R.S. Walters, M.A. Duncan, *J. Chem. Phys.* 121 (2004) 10498.
- [37] R.S. Walters, P.v.R. Schleyer, C. Corminboeuf, M.A. Duncan, *J. Am. Chem. Soc.* 127 (2005) 1100.
- [38] T.D. Jaeger, M.A. Duncan, *J. Phys. Chem. A* 109 (2005) 3311.
- [39] R.S. Walters, E.D. Pillai, M.A. Duncan, *J. Am. Chem. Soc.* 127 (2005) 16599.
- [40] R.S. Walters, E.D. Pillai, P.v.R. Schleyer, M.A. Duncan, *J. Am. Chem. Soc.* 127 (2005) 17030.
- [41] N.R. Walker, R.S. Walters, M.A. Duncan, *New J. Chem.* 29 (2005) 1495.
- [42] E.D. Pillai, T.D. Jaeger, M.A. Duncan, *J. Am. Chem. Soc.* 129 (2007) 2297.
- [43] J. Velasquez III, B. Njegic, M.S. Gordon, M.A. Duncan, *J. Phys. Chem. A* 112 (2008) 1907.
- [44] P.D. Carnegie, B. Bandyopadhyay, M.A. Duncan, *J. Phys. Chem. A* 112 (2008) 6237.
- [45] G.E. Douberly, A.M. Ricks, B.W. Ticknor, P.v.R. Schleyer, M.A. Duncan, *J. Am. Chem. Soc.* 129 (2007) 13782.
- [46] G.E. Douberly, A.M. Ricks, P.v.R. Schleyer, M.A. Duncan, *J. Chem. Phys.* 128 (2008) 021102.
- [47] G.E. Douberly, A.M. Ricks, B.W. Ticknor, W.C. McKee, P.v.R. Schleyer, M.A. Duncan, *J. Phys. Chem. A* 112 (2008) 1897.
- [48] G.E. Douberly, A.M. Ricks, B.W. Ticknor, P.v.R. Schleyer, M.A. Duncan, *J. Phys. Chem. A* 112 (2008) 4869.
- [49] J.-W. Shin, N.I. Hammer, E.G. Diken, M.A. Johnson, R.S. Walters, T.D. Jaeger, M.A. Duncan, R.A. Christie, K.D. Jordan, *Science* 304 (2004) 1137.
- [50] J. Headrick, E.G. Diken, R.S. Walters, N.I. Hammer, R.A. Christie, J. Cui, E.M. Myshakin, M.A. Duncan, M.A. Johnson, K.D. Jordan, *Science* 308 (2005) 1765.
- [51] G.E. Douberly, A.M. Ricks, B.W. Ticknor, M.A. Duncan, *Phys. Chem. Chem. Phys.* 10 (2008) 77.
- [52] G.E. Douberly, A.D. Ricks, B.W. Ticknor, M.A. Duncan, *J. Phys. Chem. A* 112 (2008) 950.
- [53] (a) L.I. Yeh, M. Okumura, J.D. Myers, J.M. Price, Y.T. Lee, *J. Chem. Phys.* 91 (1989) 7319;
(b) M. Okumura, L.I. Yeh, J.D. Myers, Y.T. Lee, *J. Phys. Chem.* 94 (1990) 3416.
- [54] T. Ebata, A. Fujii, N. Mikami, *Int. Rev. Phys. Chem.* 17 (1998) 331.
- [55] E.J. Bieske, O. Dopfer, *Chem. Rev.* 100 (2000) 3963.
- [56] W.H. Robertson, M.A. Johnson, *Annu. Rev. Phys. Chem.* 54 (2003) 173.
- [57] J.A. Kelly, W.H. Robertson, M.A. Johnson, *Chem. Phys. Lett.* 362 (2002) 255.